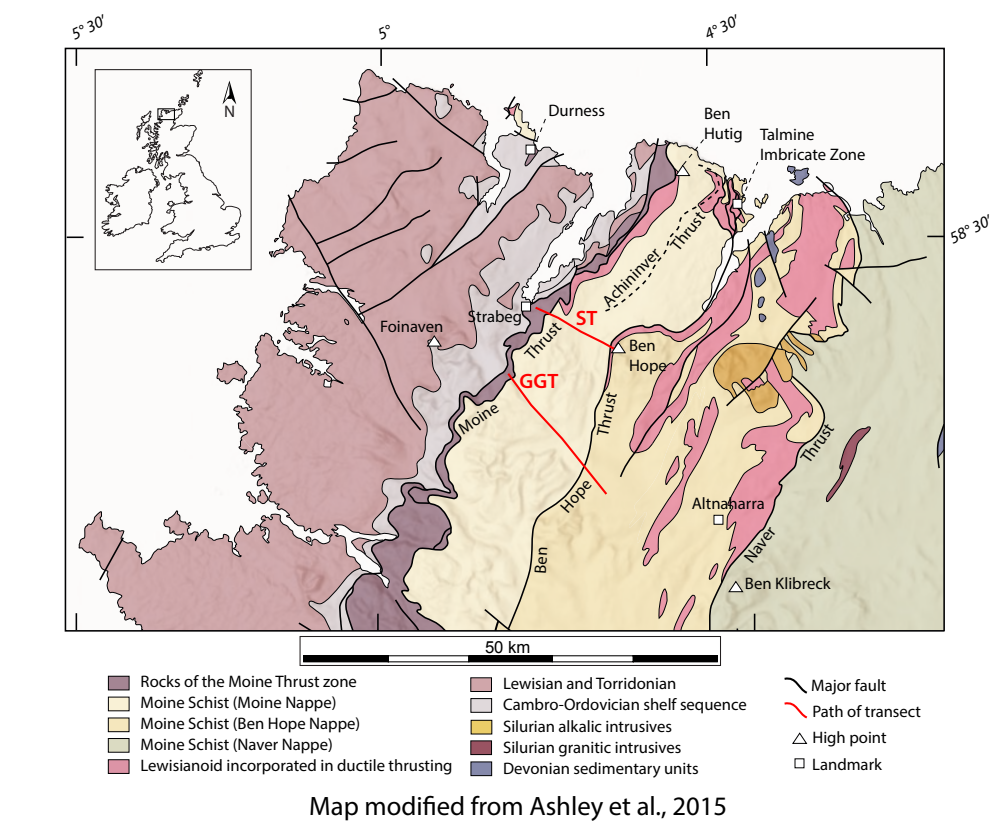


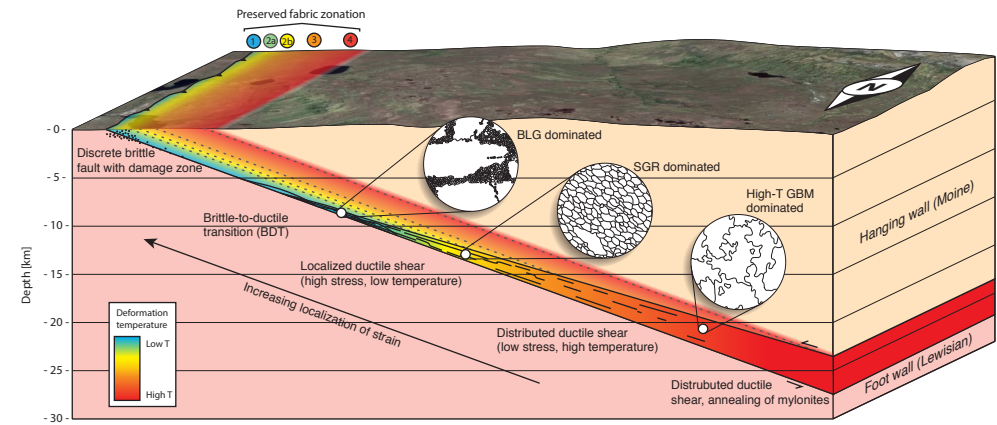
Development of interconnected fine-grained polyphase networks during progressive exhumation of a shear zone

Alexander D. Lusk^{1,2}, John P. Platt²
1 - Department of Geoscience, University of Wisconsin - Madison
2 - Department of Earth Science, University of Southern California
alusk@wisc.edu

Study area:

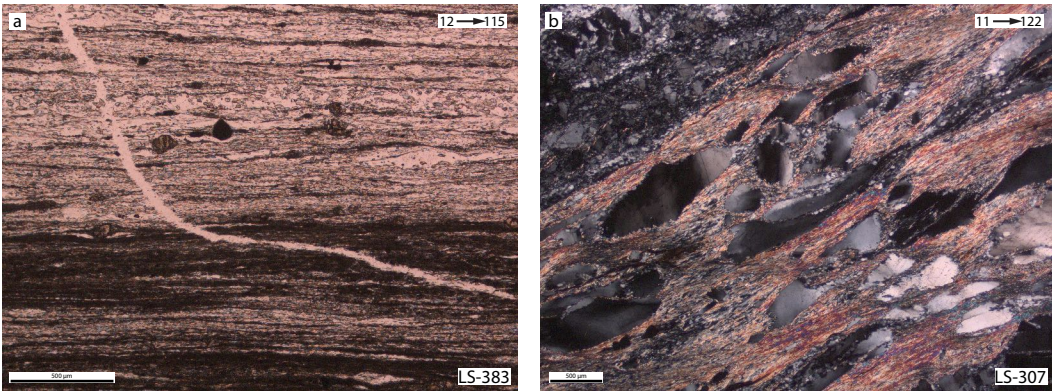


Reconstructing the shear zone at depth:



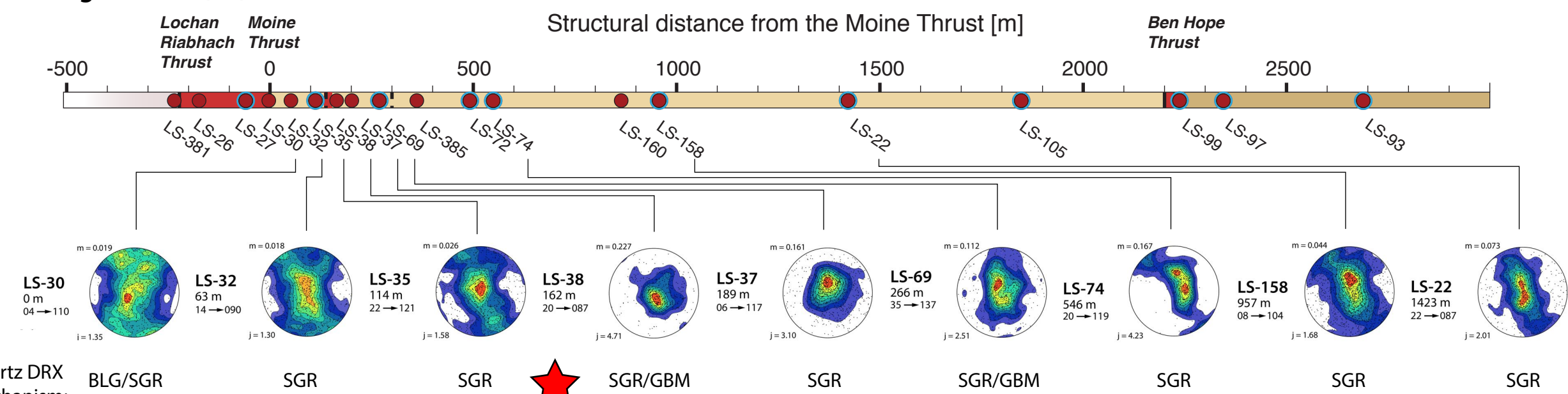
Schematic illustration of a generalized shear zone, modeled after constraints from the Moine shear zone (note that overlying and underlying thrusts are ignored for this illustration). A generalized reverse-sense shear zone localizes with decreasing depth into an anastomosing region around the brittle-to-ductile transition and finally into a discrete brittle fault with associated damage zone. Localization of strain in the deeper sections results in rocks representative of different shear zones depths (and widths) being uplifted piggy-back style along material lines (dashed). Continued movement along this zone will eventually give rise to a preserved fabric zonation preserved on the surface. Surface imagery from Google Earth.

Fine-grained polyphase layer rheology:



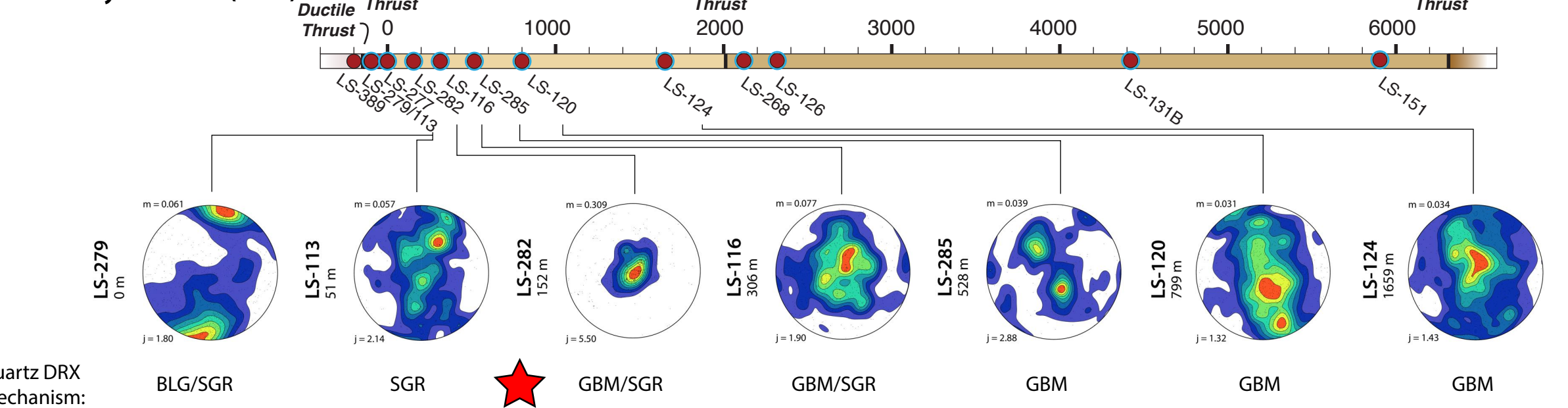
Interconnected polyphase fine-grained layers (a) and micaceous layers (b) are demonstrably weaker than the surrounding quartz. (a) cross-cutting quartz vein shows more deflection in the poly-phase layer (lower portion) compared to the quartz-rich layer (upper portion). In top-left shear, this indicates that the poly-phase region accommodated more strain than the quartz-rich region. (b) a network of interconnected micas with variably-recrystallized quartz lozenges. The largely unrecrystallized quartz indicates a strong-phase (quartz) in weak-phase (mica matrix) relationship. (a) plane polarized light, (b) cross-polarized light.

Strabeg transect (ST):



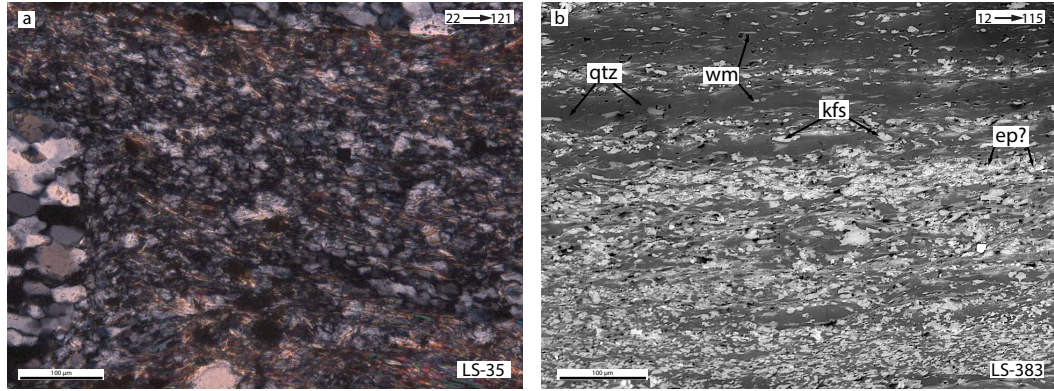
Quartz DRX mechanism: BLG/SGR SGR SGR SGR/GBM SGR SGR/GBM SGR SGR SGR
Deformation temperature* [°C]: N/D N/D 356 (+34/-33) N/D N/D 382 (+49/-57) 354 (+20/-16) 374 (+34/-34) 431 (+23/-24)
Fine-grained polyphase layers present Fine-grained polyphase layers absent

Glen Golly transect (GGT):



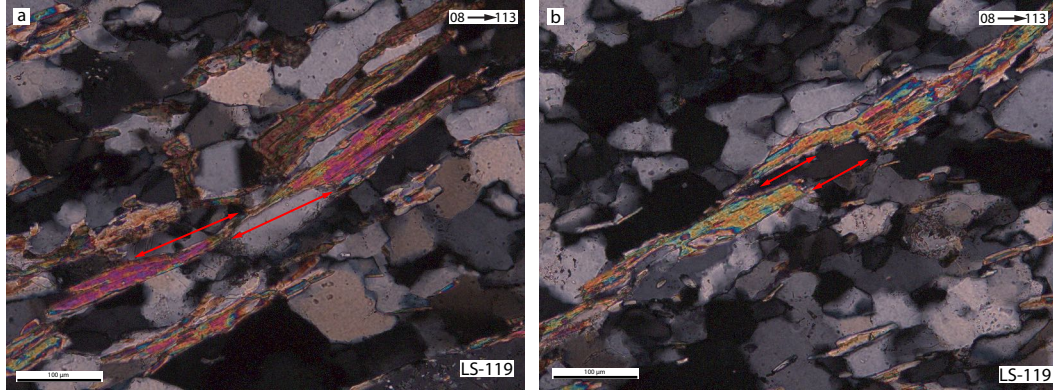
Quartz DRX mechanism: BLG/SGR SGR GBM/SGR GBM/SGR GBM GBM GBM
Deformation temperature* [°C]: 310 (+17/-17) 328 (+16/-22) 344 (+22/-21) 321 (+19/-17) N/D 371 (+19/-19) 401 (+20/-18)
Fine-grained polyphase layers present Fine-grained polyphase layers absent

Fine-grained polyphase layers:



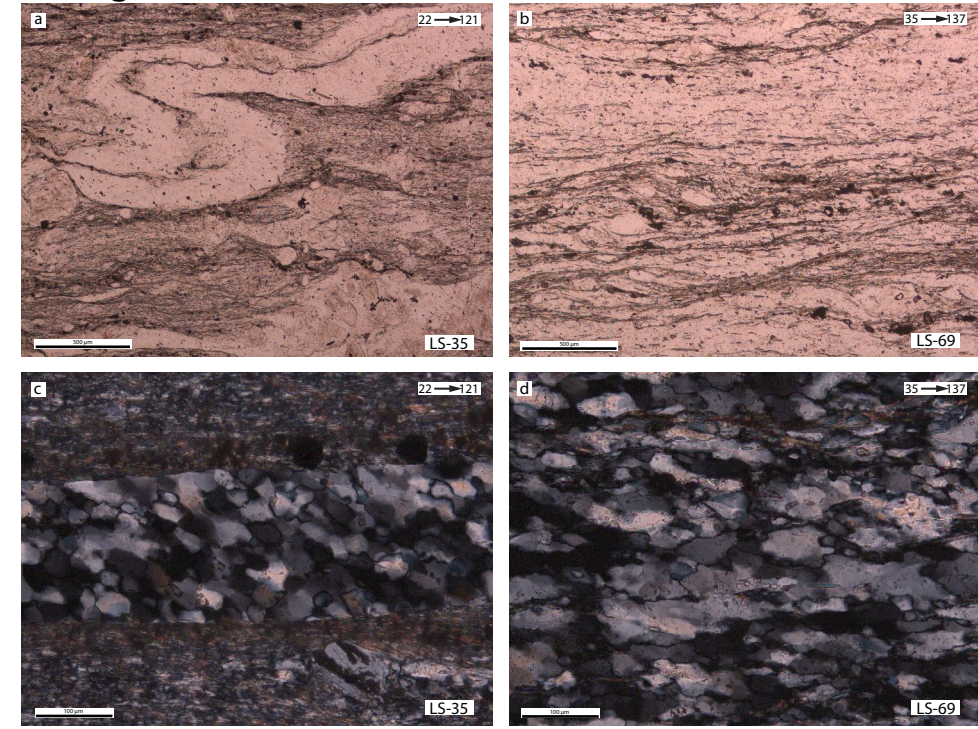
Cross-polarized optical (a) and backscatter electron (b) images of fine-grained polyphase aggregates. Both images show a mixing of quartz, micas, and feldspars into a fine-grained matrix distinct from that of pure quartz or matrix at higher structural levels. For (b), phases as follows: qtz - quartz; wm - white mica; kfs - potassic feldspar; ep? - possible epidote.

Comminution of mica:

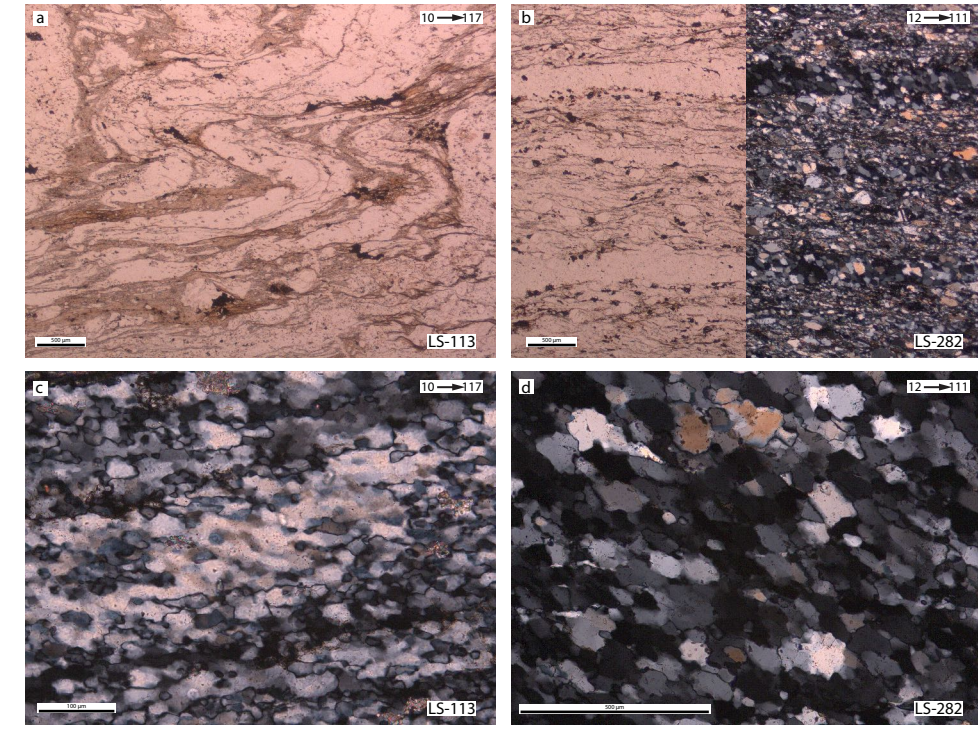


Mechanical separation of mica by fracture or dynamic recrystallization is a plausible mechanism to decrease the grain-size and grow interconnected mica networks. (a) and (b) both illustrate possible mechanical separation parallel to red arrows based on the reconstructed fit of grain boundaries. Both images in cross-polarized light, foliation inclined towards ~060.

Microstructural characterization: Strabeg transect:



Glen Golly transect:



Comparison of fine-grained polyphase dominated microstructures at structurally lower levels (a) and coarser-grained quartz-dominated microstructures with interconnected micaceous layers at structurally higher levels (b) from the Strabeg Transect (top panel) and Glen Golly Transect (lower panel). Note buckle folding in (a) indicating that the quartz vein is stronger than the surrounding fine-grained polyphase matrix. In contrast, interconnected micaceous layers in (b) form shear bands, with no significant viscosity contrast observed in the matrix. This transition coincides with a change in dominant quartz recrystallization mechanism from high-T recrystallization by GBM/SGR characterized by irregular and amoeboid grain shapes (d), to recrystallization dominated by SGR with more equant grains of roughly the same size as subgrains, and straighter grain boundaries (c).

Conclusions

(1) Quartz crystallographic preferred orientations record consistent transitions along two separate transects, each of which develops with changing temperature. These transitions record changes in the active slip systems, which we attribute to (a) a decrease in grain boundary mobility (and quartz recrystallization mechanism) due to lower deformation temperatures, and (b) finite strain. Quartz textures in the hanging wall of the Moine Thrust show extensive evidence for inheritance of grain orientations from deeper regions, indicating incomplete transitions to the easy slip system at lower structural levels (i.e. shallower regions).
(2) We postulate that transitions in easy slip system may transiently strengthen quartz aggregates, causing strain to become increasingly partitioned into phyllosilicate and polyphase layers. This partitioning could trigger the development of fine-grained polyphase interconnected weak networks, which are demonstrably weaker than pure quartz or quartz-feldspar aggregates. These weak networks likely deform by grain-size sensitive mechanisms including diffusion-accommodated grain boundary sliding and could be of first-order importance in strain localization within polyphase mylonitic and ultramylonitic rocks.

* Deformation temperature and pressure determined by Ti-in-quartz (TitaniQ) and Si-in-white mica (see Lusk and Platt, 2020)